

Structural, electrochemical and UV/VIS/NIR spectroelectrochemical properties of diastereomerically pure dinuclear ruthenium complexes based on the bridging ligand phenanthroline-5,6-diimine, and a mononuclear by-product with a peripheral isoimidazole group

Nicholas C. Fletcher, Toby C. Robinson, Andreas Behrendt, John C. Jeffery, Zoe R. Reeves and Michael D. Ward*

School of Chemistry, University of Bristol, Cantock's Close, Bristol, UK BS8 1TS.
E-mail: mike.ward@bristol.ac.uk

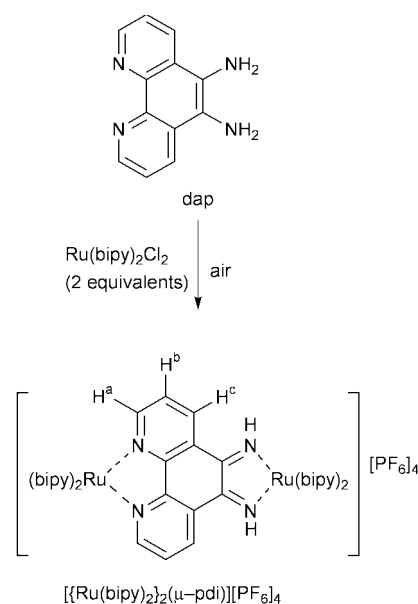
Received 5th May 1999, Accepted 2nd July 1999

Mono- and di-nuclear ruthenium(II) complexes derived from the potentially bridging ligand 5,6-diaminophenanthroline (dap) have been prepared and investigated. Reaction of dap (which has one 'bipyridyl-like' and one diamine co-ordination site) with $[\text{Ru}(\text{bipy})_2\text{Cl}_2]$ afforded $[\{\text{Ru}(\text{bipy})_2\}_2(\mu\text{-pdi})]^{4+}$, where pdi = phenanthroline-5,6-diimine, in which the diamine site has undergone a two-electron oxidation to give a quinone diimine site. The complex (as its hexafluorophosphate salt) could be separated chromatographically into its two diastereoisomers which were fully characterised independently, including the crystal structure of the homochiral diastereoisomer as its perchlorate salt. Electrochemical studies revealed six reversible reductions, of which the first two were shown by spectroelectrochemical studies to be centred on the bridging ligand (diimine/diiminosemiquinone and diiminosemiquinone/diamide couples), and the rest based on the terminal bipyridyl ligands. Although these six reductions occurred at identical potentials for both diastereoisomers, the separation between the two closely spaced $\text{Ru}^{\text{II}}\text{-Ru}^{\text{III}}$ couples varied slightly between the diastereoisomers indicating some sensitivity of delocalisation in the $\text{Ru}^{\text{II}}\text{-Ru}^{\text{III}}$ mixed-valence state to the optical configuration of the metal centres. The mononuclear complex $[\text{Ru}(\text{bipy})_2(\text{dap})]^{2+}$, in which the metal is co-ordinated at the bipyridyl site of dap with the diamine site vacant, easily reacts with acetone to give $[\text{Ru}(\text{bipy})_2\text{L}]^{2+}$ where L is a phenanthroline derivative with a peripheral isoimidazole ring derived from condensation of one equivalent of acetone with the *o*-diamine group. The electrochemical, spectroscopic and luminescence properties of $[\text{Ru}(\text{bipy})_2\text{L}]^{2+}$ are only slightly perturbed from those of $[\text{Ru}(\text{bipy})_3]^{2+}$.

Introduction

Dinuclear complexes in which polypyridylruthenium(II) fragments are connected by conjugated bridging ligands have been of recent interest for three distinct reasons. First, the photo-physical properties of multi-chromophore or chromophore-quencher complexes continue to attract attention because of their relevance to solar energy capture and artificial photosynthesis.¹ Secondly, the redox properties of such dinuclear complexes often permit the preparation of mixed-valence species in which long-distance inter-valence electron transfer may be studied as a function of the nature of the bridging ligand.² Thirdly, and of most relevance to this paper, when the complex units are chiral tris-chelates there has been much interest in either separating the diastereoisomers of the polynuclear complexes or preparing them optically pure in the first place, in order to see how the usually ignored question of isomerism affects the physico-chemical properties of the complexes.³⁻⁷

In this paper we describe the preparation of the dinuclear complex $[\{\text{Ru}(\text{bipy})_2\}_2(\mu\text{-pdi})][\text{PF}_6]_4$ (pdi = phenanthroline-5,6-diimine) in which two $\{\text{Ru}(\text{bipy})_2\}^{2+}$ fragments are connected by the pdi bridging ligand which has two inequivalent bidentate diimine chelating sites, and is derived from oxidation of (co-ordinated) 5,6-diaminophenanthroline (dap, Scheme 1).⁸ The complex has been separated chromatographically into its two diastereomeric forms, the spectroscopic, electrochemical and spectroelectrochemical properties of which have been determined. In addition one of the diastereoisomers has been crystallographically characterised, and the crystal structure of a mononuclear by-product is also described.



Scheme 1

Results and discussion

Synthesis and characterisation of $[\{\text{Ru}(\text{bipy})_2\}_2(\mu\text{-pdi})][\text{PF}_6]_4$

Our interest in dap as a bridging ligand was stimulated by the recent publication of a simple, high-yield synthesis of it starting

from 1,10-phenanthroline.⁸ Whilst dap has been used to prepare extended planar bridging ligands by condensation with quinones,^{3,9} it has not been used as a bridging ligand in its own right, in contrast to *e.g.* phenanthroline-5,6-dione which has N,N-donor and O,O-donor chelating sites.¹⁰

Reaction of dap with 2 equivalents of $[\text{Ru}(\text{bipy})_2\text{Cl}_2]$ in EtOH at reflux, followed by chromatographic purification on Sephadex SP-25 and precipitation of the complexes as their hexafluorophosphate salts, afforded some of the known⁸ orange mononuclear complex $[\text{Ru}(\text{bipy})_2(\text{dap})][\text{PF}_6]_2$ and a major purple-red product. The major product was readily identified as a dinuclear complex on the basis of its electrospray mass spectrum ($m/z = 1470$, 100% and 1325 , 50%), but the molecular weight appeared to be two mass units lower than would be expected for a dinuclear complex $[\{\text{Ru}(\text{bipy})_2\}_2(\mu\text{-dap})][\text{PF}_6]_4$ in which the bridging ligand retains the diamine nature of one of its binding sites. This suggested formation of $[\{\text{Ru}(\text{bipy})_2\}_2(\mu\text{-pdi})][\text{PF}_6]_4$ (Scheme 1), in which the diamine binding site of the bridging ligand has oxidised to the di-imino form with the concomitant loss of two protons that accompanies oxidation of the diamine to a diimine, and the two principal mass spectral peaks can be ascribed to $\{\text{M} - \text{PF}_6\}^+$ and $\{\text{M} - 2\text{PF}_6\}^+$. This behaviour is consistent with that observed by Lever and co-workers¹¹ when $[\text{Ru}(\text{bipy})_2\text{Cl}_2]$ was treated with 1,2-diaminobenzene and its substituted derivatives; although the 1,2-diaminobenzene could co-ordinate in its reduced diamino form when the reaction was carried out in an inert atmosphere, exposure to oxygen quickly resulted in 2-electron oxidation and deprotonation to give co-ordinated 1,2-benzoquinone-diimine. That similar behaviour is occurring here is apparent not only from the mass spectrum, but also from the electrochemical, spectroscopic and crystallographic properties of the complex (see later).

Since the two metal centres of the dinuclear complex are chiral and inequivalent to one another, we expect four stereoisomers $\Delta\Delta$, $\Delta\Lambda$, $\Lambda\Delta$ and $\Lambda\Lambda$ to form (see ref. 4 for illustrations of these). These can be grouped into two diastereomeric pairs, $\Delta\Delta/\Lambda\Lambda$ and $\Delta\Lambda/\Lambda\Delta$. Keene and co-workers⁴ recently described a chromatographic method for the separation of such diastereoisomers using cation-exchange chromatography on Sephadex SP-25 eluting with an aqueous solution of sodium toluene-*p*-sulfonate, and we were able to separate $[\{\text{Ru}(\text{bipy})_2\}_2(\mu\text{-pdi})][\text{PF}_6]_4$ into its two diastereoisomers in this way. We could not obtain X-ray quality crystals of either diastereoisomer as the hexafluorophosphate salt, despite several attempts. Accordingly small amounts of each were converted into the perchlorate salts, and X-ray quality crystals of the slower-eluting diastereoisomer of $[\{\text{Ru}(\text{bipy})_2\}_2(\mu\text{-pdi})]^{4+}$ (as its perchlorate salt) were obtained by slow evaporation of the complex from aqueous MeCN.

The crystal structure (Fig. 1; see also Table 1) showed this complex to be the homochiral $\Delta\Delta/\Lambda\Lambda$ diastereoisomer, with both enantiomers present in the achiral crystal. The structural determination was complicated by substantial disorder which was however successfully resolved (see Experimental section). Both metal complex termini have the expected pseudo-octahedral geometries with unremarkable metrical parameters. The most significant feature of the structure (apart from determination of which diastereoisomer it is) is the fact that the Ru–N (bipyridyl) and Ru–N (imine) distances are essentially identical at *ca.* 2.05 Å. This confirms that the bridging ligand is in the oxidised diimine form, as the Ru–N distance to an aromatic amine is typically *ca.* 2.2 Å.¹² The fact that the two metal fragments are in effectively identical co-ordination environments allows this disorder of the bridging ligand, because inversion of the bridging ligand, switching over of the binding sites, causes minimum perturbation in the rest of the structure. In fact only four of the carbon atoms in the bridging ligand need to be disordered over two sites (Fig. 2) to interconvert the positions of the bipyridyl and diimine binding sites, with all

Table 1 Selected bond lengths (Å) and angles (°) for $[\{\text{Ru}(\text{bipy})_2\}_2(\mu\text{-pdi})][\text{ClO}_4]_4 \cdot 2.5\text{H}_2\text{O}$

Ru(1)–N(121)	2.013(7)	Ru(2)–N(101)	2.038(7)
Ru(1)–N(124)	2.019(7)	Ru(2)–N(111)	2.043(7)
Ru(1)–N(11)	2.047(8)	Ru(2)–N(71)	2.058(8)
Ru(1)–N(41)	2.051(7)	Ru(2)–N(61)	2.062(8)
Ru(1)–N(31)	2.065(7)	Ru(2)–N(51)	2.067(8)
Ru(1)–N(21)	2.068(7)	Ru(2)–N(81)	2.073(7)
N(121)–Ru(1)–N(124)	78.1(3)	N(101)–Ru(2)–N(111)	78.8(3)
N(121)–Ru(1)–N(11)	98.2(3)	N(101)–Ru(2)–N(71)	97.0(3)
N(124)–Ru(1)–N(11)	91.2(3)	N(111)–Ru(2)–N(71)	86.4(3)
N(121)–Ru(1)–N(41)	88.8(3)	N(101)–Ru(2)–N(61)	94.9(3)
N(124)–Ru(1)–N(41)	96.0(3)	N(111)–Ru(2)–N(61)	172.7(3)
N(11)–Ru(1)–N(41)	170.8(3)	N(71)–Ru(2)–N(61)	98.1(3)
N(121)–Ru(1)–N(31)	94.1(3)	N(101)–Ru(2)–N(51)	91.1(3)
N(124)–Ru(1)–N(31)	170.8(3)	N(111)–Ru(2)–N(51)	97.2(3)
N(11)–Ru(1)–N(31)	94.8(3)	N(71)–Ru(2)–N(51)	171.7(3)
N(41)–Ru(1)–N(31)	78.7(3)	N(61)–Ru(2)–N(51)	79.2(4)
N(121)–Ru(1)–N(21)	174.8(3)	N(101)–Ru(2)–N(81)	174.3(3)
N(124)–Ru(1)–N(21)	97.8(3)	N(111)–Ru(2)–N(81)	97.4(3)
N(11)–Ru(1)–N(21)	78.6(3)	N(71)–Ru(2)–N(81)	78.4(3)
N(41)–Ru(1)–N(21)	94.8(3)	N(61)–Ru(2)–N(81)	89.2(3)
N(31)–Ru(1)–N(21)	90.2(3)	N(51)–Ru(2)–N(81)	93.6(3)

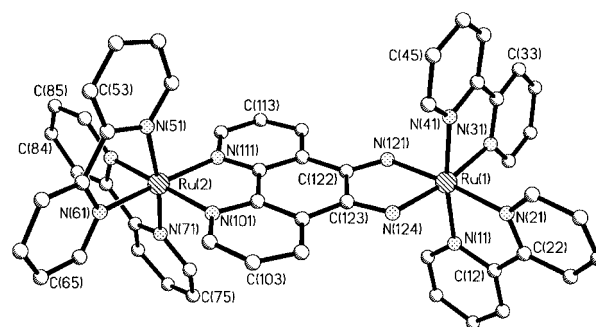


Fig. 1 Crystal structure of the complex cation of $[\{\text{Ru}(\text{bipy})_2\}_2(\mu\text{-pdi})][\text{ClO}_4]_4 \cdot 2.5\text{H}_2\text{O}$ (homochiral diastereoisomer).

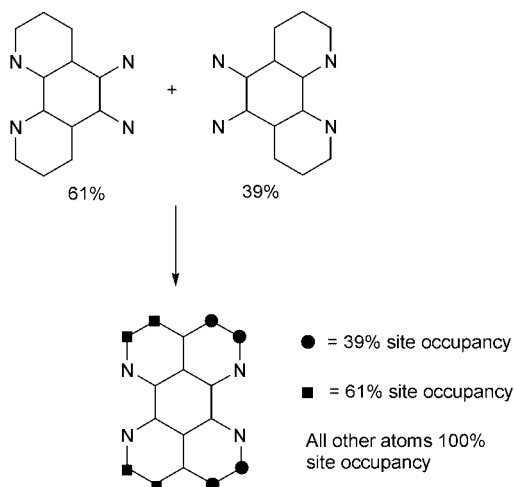


Fig. 2 Schematic illustration of the disorder involving the bridging ligand in the crystal structure of $[\{\text{Ru}(\text{bipy})_2\}_2(\mu\text{-pdi})][\text{ClO}_4]_4$.

other atom positions being common to both components of the disorder. There is also substantial disorder of the perchlorate anions (see Experimental section for full details).

Having identified the two diastereoisomers as homochiral $\Delta\Delta/\Lambda\Lambda$ (slower-eluting) and heterochiral $\Delta\Lambda/\Lambda\Delta$ (faster-eluting), we examined their ¹H NMR spectra (Fig. 3). With the aid of two-dimensional (COSY) methods the spectra could be separated into four sets of four resonances (for pyridyl rings, **a–d**), and one set of three resonances (for the bridging ligand, BL), although it is not possible to ascribe each set of four resonances to a particular pyridyl ring. The presence of only

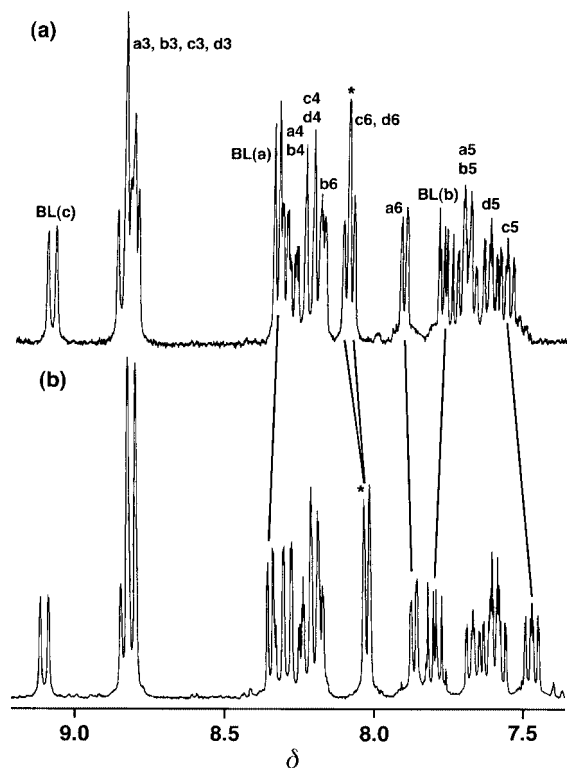


Fig. 3 The ^1H NMR spectra (CD_3CN , 300 MHz) of the two diastereoisomers of $[\{\text{Ru}(\text{bipy})_2\}_2(\mu\text{-pdi})][\text{PF}_6]_2$: (a) heterochiral diastereoisomer; (b) homochiral diastereoisomer. The four magnetically inequivalent pyridyl rings are a–d, such that c4 denotes H^4 of ring c, and the bridging ligand (BL) protons a, b and c are as shown in Schemes 1 and 2.

four sets of pyridyl signals, each corresponding to two equivalent pyridyl rings, is because of the presence of a C_2 axis which passes through both Ru atoms and which bisects the bridging ligand. The two bipyridyl ligands attached to each metal ion are accordingly magnetically equivalent. The imine NH protons in each case appeared as a broad singlet at δ ca. 14.3 with the correct integral value. Comparison of the two spectra shows that although they are generally similar there are some small but significant differences between them. For example, the signal labelled * in Fig. 3 corresponds to the H^6 protons of two of the pyridyl rings. For the homochiral complex the two H^6 resonances are accidentally degenerate and therefore superimposed, whereas for the heterochiral complex the two doublets have separated just enough to give the appearance of a triplet and have moved by on average 0.05 ppm.

Synthesis, crystal structure and properties of the mononuclear complex $[\text{Ru}(\text{bipy})_2\text{L}][\text{PF}_6]_2$

The orange by-product produced in the above reaction was identified from its mass spectrum as the mononuclear complex $[\text{Ru}(\text{bipy})_2(\text{dap})][\text{PF}_6]_2$, in which the $\{\text{Ru}(\text{bipy})_2\}^{2+}$ fragment is attached to the phenanthroline binding site of dap to give a $[\text{Ru}(\text{bipy})_3]^{2+}$ -like core with a pendant diamino group.⁸ However recrystallisation from acetone–diethyl ether afforded an orange material whose electrospray mass spectrum showed that the mass of the complex cation was 38 units higher than expected, and the ^1H NMR spectrum showed a singlet (relative intensity 6 H) at δ 1.64, in addition to the expected eleven signals (relative intensity 2 H each) in the aromatic region. These observations are consistent with reaction of the pendant diamine site with the acetone used in the recrystallisation to give a 2,2-dimethyl-2H-imidazole (an ‘isoimidazole’, Scheme 2); a similar reaction between 1,2-diaminobenzene and cyclohexane was reported a while ago.¹³ Further recrystallisation from MeCN–ether afforded X-ray quality crystals.

Table 2 Selected bond lengths (\AA) and angles ($^\circ$) for $[\text{Ru}(\text{bipy})_2\text{L}][\text{PF}_6]_2 \cdot 2\text{MeCN}$

Ru–N(11)	2.058(2)	C(41)–C(41A)	1.482(7)
Ru–N(21)	2.063(3)	N(42)–C(43)	1.483(4)
Ru–N(31)	2.077(2)	C(43)–C(44)	1.519(5)
C(41)–N(42)	1.288(4)	C(35)–C(41)	1.454(4)
N(11)–Ru–N(11A)	172.7(2)	N(21)–Ru–N(31A)	173.34(10)
N(11)–Ru–N(21)	78.79(11)	N(11)–Ru–N(31)	88.50(10)
N(11)–Ru–N(21A)	95.98(10)	N(21)–Ru–N(31)	96.20(9)
N(21)–Ru–N(21A)	89.52(14)	N(31A)–Ru–N(31)	78.30(14)
N(11)–Ru–N(31A)	97.16(10)		
N(42)–C(41)–C(35)	128.6(3)	N(42)–C(43)–N(42A)	108.3(4)
N(42)–C(41)–C(41A)	111.0(2)	N(42)–C(43)–C(44A)	109.8(2)
C(35)–C(41)–C(41A)	120.4(2)	N(42)–C(43)–C(44)	109.0(2)
C(41)–N(42)–C(43)	104.9(3)	C(44A)–C(43)–C(44)	110.9(4)

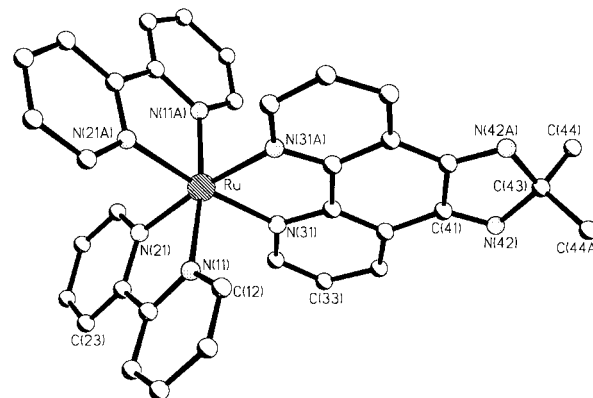
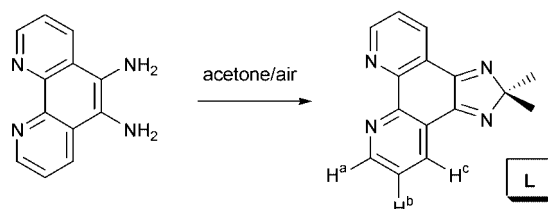


Fig. 4 Crystal structure of the cation of $[\text{Ru}(\text{bipy})_2\text{L}][\text{PF}_6]_2 \cdot 2\text{MeCN}$.



Scheme 2 Preparation of the isoimidazole-based derivative L, showing the ^1H NMR labelling scheme.

The formulation of the compound was confirmed by the crystal structure (Fig. 4, Table 2), which shows the complex to have the usual $\{\text{Ru}(\text{bipy})_3\}^{2+}$ -type core with a planar, 5-membered isoimidazole ring fused on to what used to be the diamino-phenanthroline ligand. The molecule has crystallographic C_2 symmetry, with the C_2 axis passing through the Ru atom and also C(43). That the C–N linkages in the five-membered ring are alternately double and single is clear from their lengths: the C(41)–N(42) separation (double bond) is 1.288(4) \AA , whereas the N(42)–C(43) separation (single bond) is 1.483(4) \AA . Also, the C(41)–C(41A) separation at 1.482(7) \AA is indicative of a single C–C bond, as expected. In contrast the 1.5-order bonds in the bipyridyl ligands all lie in the range 1.34–1.40 \AA . The geometry about the metal centre, with Ru–N distances in the range 2.06–2.08 \AA and ligand bite angles of just under 80° , is unremarkable. We note that a similar structure has been reported recently containing a normal imidazole group (rather than an isoimidazole) fused in the same way to a phenanthroline backbone.¹⁴

The spectroscopic and electrochemical properties of $[\text{Ru}(\text{bipy})_2\text{L}][\text{PF}_6]_2$ are generally similar to those of $[\text{Ru}(\text{bipy})_3]^{2+}$. Cyclic voltammetry in MeCN shows the expected reversible $\text{Ru}^{\text{II}}\text{--Ru}^{\text{III}}$ couple at +0.96 V vs. the ferrocene–ferrocenium couple ($\text{Fc}\text{--Fc}^+$). ‘Reversible’ is taken to mean that the anodic

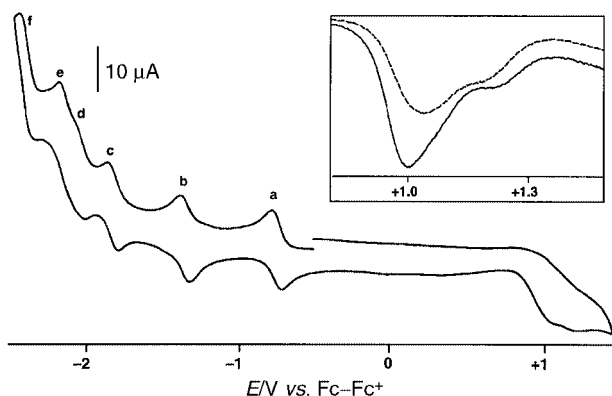


Fig. 5 Cyclic voltammogram of $[\{\text{Ru}(\text{bipy})_2\}_2(\mu\text{-pdi})][\text{PF}_6]_4$ (heterochiral isomer) in MeCN at a scan rate of 0.2 V s^{-1} . Processes (a) and (b) are the diimine/diiminosemiquinone and diiminosemiquinone/diamide processes of the bridging ligand; (c)–(f) are bipy-centred reductions. The inset shows square-wave voltammograms of the heterochiral (solid line) and homochiral (dashed line) isomers in the region of the metal-centred $\text{Ru}^{\text{II}}\text{--Ru}^{\text{III}}$ couples.

and cathodic peak currents are equal, and the peak–peak separation is 70–80 mV at a scan rate of 200 mV s^{-1} . This redox potential is about 70 mV more positive than the same couple of $[\text{Ru}(\text{bipy})_3]^{2+}$ under the same conditions,¹⁵ because the weak electron-withdrawing effect of the electronegative substituents at N stabilises the lower oxidation state. There are also three reversible one-electron ligand-centred reductions, at -1.39 , -1.84 and $-2.06 \text{ V vs. Fc-Fc}^+$, of which we assign the first to the relatively electron-deficient ligand L and the subsequent two to the two bipyridyl ligands.¹⁵ The electronic spectrum has the lowest-energy ¹MLCT transition at $\lambda_{\text{max}} = 430 \text{ nm}$ ($\epsilon = 10\,000 \text{ dm}^3 \text{ mol}^{-1} \text{ cm}^{-1}$) in addition to the usual intense ligand-centred transitions in the UV region at $\lambda_{\text{max}} = 286$ ($\epsilon = 40\,000$) and 241 nm ($\epsilon = 30\,000 \text{ dm}^3 \text{ mol}^{-1} \text{ cm}^{-1}$). Irradiation of the ¹MLCT transition in aerated MeCN at room temperature results in luminescence, which we assume to be from the ³MLCT excited state,¹⁵ at 654 nm ($\phi = 0.012$).

We examined the reaction of free dap with acetone and found that in the presence of air it gave at room temperature the ligand L in reasonable yield. Reaction of L with $[\text{Ru}(\text{bipy})_2\text{Cl}_2]$ afforded $[\text{Ru}(\text{bipy})_2\text{L}][\text{PF}_6]_2$ in high yield, and the properties of the complex obtained by this route were identical to those from the material obtained by recrystallisation of $[\text{Ru}(\text{bipy})_2(\text{dap})][\text{PF}_6]_2$ from acetone. Although this complex $[\text{Ru}(\text{bipy})_2\text{L}][\text{PF}_6]_2$ was an accidental by-product of our attempts to make the dinuclear complex, the ease with which it formed in the presence of acetone suggests that reaction of the mononuclear precursor $[\text{Ru}(\text{bipy})_2(\text{dap})]^{2+}$ with compounds containing two or more carbonyl groups (e.g. terephthalaldehyde) could be a simple route to multi-chromophoric complexes, and we are currently investigating this possibility.

Electrochemical studies on the two diastereoisomers of $[\{\text{Ru}(\text{bipy})_2\}_2(\mu\text{-pdi})][\text{PF}_6]_4$

Cyclic voltammetric studies on each diastereoisomer of $[\{\text{Ru}(\text{bipy})_2\}_2(\mu\text{-pdi})][\text{PF}_6]_4$ showed that the potentials of their redox couples are very similar, see Fig. 5. There are two overlapping oxidations at positive potentials which cannot be resolved by cyclic voltammetry, but square-wave voltammetry allows resolution of the two processes whose peak potentials are at $+1.00$ and $+1.21 \text{ V vs. Fc-Fc}^+$ for the heterochiral diastereoisomer, and $+1.04$ and $+1.17 \text{ V}$ for the homochiral diastereoisomer. By comparison with the properties of the mononuclear model complexes $[\text{Ru}(\text{bipy})_3]^{2+}$ and $[\text{Ru}(\text{bipy})_2(\text{bqdi})]^{2+}$ (bqdi = 1,2-benzoquinone diimine), we ascribe these to metal-centred $\text{Ru}^{\text{II}}\text{--Ru}^{\text{III}}$ couples.^{11,15} It is noteworthy that the redox separation is 210 mV in the former case and 130 mV in

the latter. Given the close overlap of the two processes (Fig. 5), and the fact that one of them is irreversible (shown by the low intensity of the return wave on the cyclic voltammogram), these figures are subject to an uncertainty larger than the normal $\pm 10 \text{ mV}$; but even so it appears that the extent of metal–metal interaction is slightly different in the two diastereoisomers. Any contributions to these redox separations from (i) through-space electrostatic interactions and (ii) the electronic inequivalence of the two binding sites of the bridging ligand will be the same in each case, so the difference between the two $\Delta E_{1/2}$ values represents a genuine difference in the electronic coupling between the metal centres arising from the different optical configurations of the metal centres. This phenomenon has also been observed recently by Keene and co-workers⁵ in related dinuclear ruthenium complexes bridged by 2,2'-azobispyridine.†

The voltammograms of the two diastereoisomers also show six redox couples at negative potentials, which are ascribed to successive one-electron reductions of the ligands. Their one-electron nature is apparent from their equal intensities in the square-wave voltammogram and the peak–peak separations of 70–80 mV of those (the first three) that are clearly resolved. The fourth and fifth reduction waves are closely overlapping and their peak potentials were determined from the square-wave voltammogram in which two maxima were just resolved. The chemical reversibility of the first five reductions was established spectroelectrochemically (see below). These processes may again be assigned by comparison with the electrochemical properties of $[\text{Ru}(\text{bipy})_3]^{2+}$ and $[\text{Ru}(\text{bipy})_2(\text{bqdi})]^{2+}$.^{11,15} The four most negative redox couples, at -1.83 , -2.04 , -2.15 and $-2.41 \text{ V vs. Fc-Fc}^+$, we ascribe to the four terminal bipyridyl ligands. The two less negative processes at -0.73 and $-1.35 \text{ V vs. Fc-Fc}^+$ in contrast we ascribe to the stepwise reduction of the diimine fragment to the diiminosemiquinone monoanion and then the diamide dianion,¹¹ in a manner analogous to reduction of neutral quinone to a semiquinone monoanion and then a catecholate dianion. The potentials of the bridging-ligand centred couples may be compared to those of the mononuclear model complex $[\text{Ru}(\text{bipy})_2(\text{bqdi})]^{2+}$ which occur at $+0.08$ and -0.69 V vs. SCE in MeCN; even allowing for the ca. 0.4 V conversion factor between the SCE and Fc-Fc^+ reference potentials, it is clear that reduction of the bridging ligand of $[\{\text{Ru}(\text{bipy})_2\}_2(\mu\text{-pdi})][\text{PF}_6]_4$ is more difficult than reduction of the mononuclear complex $[\text{Ru}(\text{bipy})_2(\text{bqdi})]^{2+}$. This may be ascribed to the lack of delocalisation between the diimine and bipyridyl parts of the bridging ligand, such that reduction of the diimine part does not benefit from stabilisation provided by delocalisation over an extended aromatic network, whereas in bqdi the imine groups are part of a more delocalised π -system. Recently Launay and co-workers¹⁶ showed that for tetrapyrido[3,2-*a*:2'-*a*:3'-*c*:3'-*c*:2''-*h*:2''-*h*:2''-*j*]phenazine (tpphz), a bridging ligand prepared from condensation of dap with phenanthroline-5,6-dione, the terminal bipyridyl and central phenazine units are electronically isolated with molecular orbitals localised on one part or the other but not spanning both.¹⁶

† One of the referees correctly pointed out that since the second oxidation is not fully reversible the peak potential observed in the square-wave voltammogram is not the exact thermodynamic redox potential. If the rates of the following decomposition processes are different between the two diastereoisomers then the apparent peak potential for the second process would be shifted by a different amount in each case, which could account for the apparent difference in $\Delta E_{1/2}$ values. Given however that others have shown that genuine differences in electrochemical properties can occur between diastereoisomers (ref. 5), and that we have no reason to suppose that there is a significant difference between the oxidation-induced chemical reactions for the two diastereoisomers, we incline to the opinion that our measurements are evidence for a genuine (albeit small) variation in $\Delta E_{1/2}$ between the two diastereoisomers.

Table 3 Electronic spectra of $[\{\text{Ru}(\text{bipy})_2\}_2(\mu\text{-pdi})][\text{PF}_6]_4$ ($[\text{M}]^{4+}$; homochiral diastereoisomer) in MeCN at 243 K

Oxidation level	$\lambda_{\text{max}}/\text{nm}$ ($10^{-3} \epsilon/\text{dm}^3 \text{mol}^{-1} \text{cm}^{-1}$)						
$[\text{M}]^{4+}$		526 (24) ^a		420 (16) ^b		282 (88) ^c	242 (62) ^c
$[\text{M}]^{3+}$		648 (13) ^d		457 (21) ^b		289 (95) ^c	243 (53) ^c
$[\text{M}]^{2+}$	1180 (8) ^e			444 (25) ^b		291 (97) ^c	243 (55) ^c
$[\text{M}]^+$	1180 (8) ^e	531 (21) ^f	495 (19) ^f	434 (24) ^b	366 (27) ^f	294 (82) ^c	240 (53) ^c
$[\text{M}]^-$	1180 (8) ^e	543 (24) ^f	510 (22) ^f	439 (21) ^b	358 (41) ^f	321 (48) ^c	238 (45) ^c

^a Ru→diimine MLCT. ^b Ru→bipy MLCT. ^c Bipy-centred $\pi \rightarrow \pi^*$ transition. ^d Ru→diiminosemiquinone MLCT. ^e Diamide→diimine charge transfer within the bridging ligand. ^f $\pi \rightarrow \pi^*$ Transition of bipy radical anions.

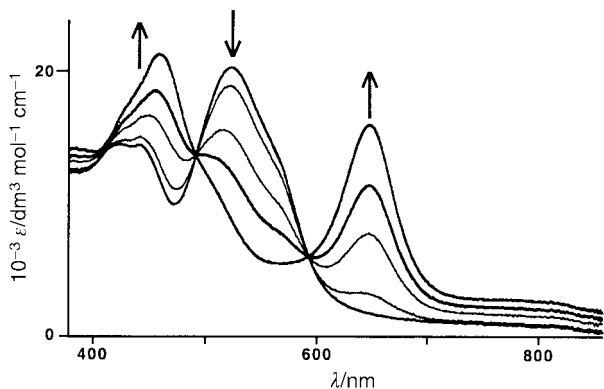


Fig. 6 Electronic spectra of $[\{\text{Ru}(\text{bipy})_2\}_2(\mu\text{-pdi})][\text{PF}_6]_4$ ($[\text{M}]^{4+}$) and its first reduction product $[\text{M}]^{3+}$, showing the replacement of the Ru→diimine MLCT transition at 526 nm by a Ru→diiminosemiquinone transition at 648 nm.

Spectroelectrochemical studies on the reduced forms of the two diastereoisomers of $[\{\text{Ru}(\text{bipy})_2\}_2(\mu\text{-pdi})][\text{PF}_6]_4$

Given the slight difference between the $\text{Ru}^{\text{II}}\text{-Ru}^{\text{III}}$ redox potentials for the two diastereoisomers of $[\{\text{Ru}(\text{bipy})_2\}_2(\mu\text{-pdi})][\text{PF}_6]_4$, we were interested to see if any difference could also be detected in their electronic spectra. Accordingly we performed a spectroelectrochemical examination of each isomer spanning six oxidation states: the parent $[\{\text{Ru}(\text{bipy})_2\}_2(\mu\text{-pdi})]^{4+}$ state, the mono- and di-reduced states where the reductions are centred on the bridging ligand, and then up to the fivefold-reduced state in which three of the bipy ligands have also been reduced. Examination of the oxidised states was not possible because the two oxidations are very close together and one of them is irreversible, and examination of the final reduced state (following the last bipy-centred reduction) was not attempted because of its extreme negative potential which is close to the solvent/base electrolyte breakdown. The results are summarised in Table 3; see also Figs. 6–8.

The electronic spectrum of heterochiral $[\{\text{Ru}(\text{bipy})_2\}_2(\mu\text{-pdi})]^{4+}$ (Fig. 6) may be assigned by comparison with reference to the appropriate mononuclear complexes, as we did for the electrochemical studies. The lowest-energy transition at 526 nm is the Ru[d(π)→diimine(π^*)] metal-to-ligand charge transfer (MLCT), which for comparison occurs at 515 nm for mononuclear $[\text{Ru}(\text{bipy})_2(\text{bqdi})]^{2+}$.¹¹ The broad area of absorbance between 400 and 460 nm, with a barely resolved maximum at 420 nm, is ascribed to the Ru[d(π)→bipy(π^*)] MLCT transitions involving both metal fragments.^{11,15} The UV region of the spectrum contains the usual intense ligand-centred transitions at 282 and 242 nm. Excitation of the complex at 420 nm in MeCN solution at room temperature produced no detectable luminescence.

The changes of the spectra during the first two reductions are, with one significant exception, very similar to those which were observed during reduction of mononuclear $[\text{Ru}(\text{bipy})_2(\text{bqdi})]^{2+}$; viz. the MLCT transition at the diimine site is red-shifted from 523 nm to 648 nm following the first reduction to the diiminosemiquinone state (Fig. 6), and then disappears on the second reduction to the diamide dianion (Fig. 7).¹¹ In

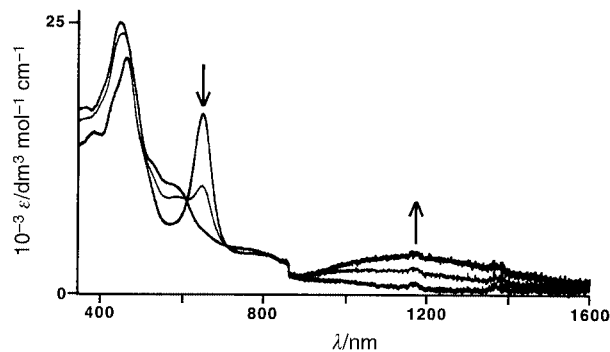


Fig. 7 Electronic spectra recorded during reduction of $[\text{M}]^{3+}$ to $[\text{M}]^{2+}$, showing collapse of the Ru→diiminosemiquinone transition at 648 nm, and the appearance of the diamide→diimine *intra*-ligand charge transfer at 1180 nm.

contrast the Ru→bipy MLCT transition is scarcely affected. This shows that (i) these first two reductions are indeed associated with reduction of the diimine site, and (ii) the diimine and bipyridyl sites are nearly electronically decoupled.¹⁶ The exception referred to above is a broad transition at 1180 nm which appears following the second reduction to the diamide dianion (Fig. 7), and which has no counterpart in the spectra of either of the mononuclear component parts. It must therefore be an ‘inter-component’ transition, and we assign it to a diamide→bipy charge-transfer transition *within the bridging ligand*, i.e. an electron transfer from a high-energy orbital localised on the reduced diamide fragment of the bridging ligand to a low-energy π^* orbital localised on the bipy fragment of the bridging ligand. There are three factors which support this assignment in addition to the fact that such a transition does not occur in the mononuclear model complexes. First, a related transition has been observed by Auburn and Lever¹⁷ between the (reduced) diiminosemiquinone and non-reduced diimine termini of a mixed-valence bridging ligand in which the valences were localised. Secondly, this transition may be considered analogous to the catecholate→bipy *inter*-ligand transitions that are well known in complexes of the type $[\text{M}(\text{bipy})(\text{cat})]$ ($\text{M} = \text{Pd}$ or Pt).¹⁸ Finally, its appearance is consistent with the molecular orbital calculations of Launay and co-workers¹⁶ which show the localisation of the molecular orbitals on dap-derived ligands, such that a description diimide→bipy (rather than delocalised $\pi \rightarrow \pi^*$) is reasonable for this *intra*-ligand transition.

Further reduction (Fig. 8) results in a decrease in intensity of the bipy-centred $\pi \rightarrow \pi^*$ transition at *ca.* 290 nm and the corresponding appearance of new transitions at 320 nm (shoulder), 366, 495 and 531 nm (the Ru→bipy MLCT transition is still also visible at 434 nm). This behaviour is exactly consistent with reduction of a terminal bipy ligand to give a radical anion; for example stepwise reduction of the bipy ligands of $[\text{Ru}(\text{bipy})_3]^{2+}$ results in the ligand-centred transition in the UV region being red-shifted from 286 to 336 nm, and the appearance of a series of closely spaced maxima from a new $\pi \rightarrow \pi^*$ transition of the (bipy)^{•-} ligand at around 500 nm.¹⁹ Finally we performed a further two-electron reduction to give

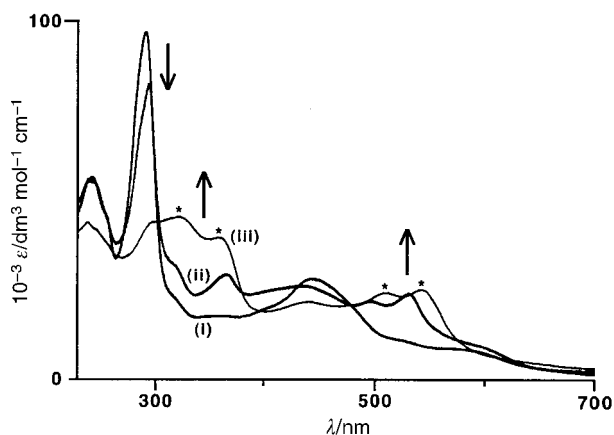


Fig. 8 Electronic spectra of (i) $[M]^{2+}$, (ii) $[M]^+$ and (iii) $[M]^{•-}$, showing the effects of reductions centred on the terminal bipyridyl ligands, in particular the disappearance of the bipy-centred $\pi \rightarrow \pi^*$ transition at *ca.* 290 nm and the appearance of several $\pi \rightarrow \pi^*$ transitions associated with the $[bipy]^{•-}$ radical anions (labelled *).

the 5-fold reduced species (the fourth and fifth reductions are too close together to perform each reduction separately). The changes that occur on reduction of two more bipy ligands are similar to those which accompanied the first bipy-based reduction, *viz.* further collapse of the bipy-centred transition at *ca.* 290 nm and an increase in intensity of the new transitions that have been identified as being associated with the $(bipy)^{•-}$ ligands, and the spectrum of this compound is strikingly similar to that of the reduced forms of $[Ru(bipy)_3]^{2+}$.¹⁹

The spectroscopic behaviour of the homochiral isomer showed no significant differences; the spectra are almost superimposable in all oxidation states. This is consistent with the observation that the redox potentials of these ligand-centred processes are identical (within the limits of accuracy of our measurements). Although we might expect to see differences in the spectra of the oxidised forms, particularly the mixed-valence state, the irreversibility of the oxidation behaviour precludes such a study.

Conclusion

Reaction of the bridging ligand dap with $[Ru(bipy)_2Cl_2]$ affords the dinuclear complex $[Ru(bipy)_2]_2(\mu\text{-pdi})[PF_6]_4$ in which the diamine site of the bridging ligand has oxidised to the diimine state with loss of two protons. The complex could be separated into its diastereoisomers, which showed a small but significant difference between their metal-based redox potentials, indicating that the metal–metal coupling is slightly sensitive to the different optical configurations of the metal centres. The six ligand-centred reductions are however essentially identical for the two diastereoisomers. Spectroelectrochemical studies of the reduced forms of $[Ru(bipy)_2]_2(\mu\text{-pdi})[PF_6]_4$ (both diastereoisomers separately) revealed that the first two are the diimine/diiminosemiquinone and diiminosemiquinone/diamide couples based on the bridging ligand, with the third and subsequent processes being based on the terminal bipyridyl ligands; there were no significant differences between the electronic spectra of the two diastereoisomers in any of the oxidation states examined.

The mononuclear complex $[Ru(bipy)_2(dap)][PF_6]_2$ was found to undergo a facile reaction with acetone in the presence of air to give $[Ru(bipy)_2L][PF_6]_2$ containing an isoimidazole group attached to the phenanthroline ligand. The free ligand dap was also found to react with acetone in the same way to give L.

Experimental

General details

Instrumentation used for routine spectroscopic and electro-

chemical studies has been described previously.²⁰ Spectroelectrochemical measurements were carried out using a home-built OTTLE (optically transparent thin layer electrode) cell mounted in the sample compartment of a Perkin-Elmer Lambda 19 spectrophotometer, as described in detail previously;²⁰ all measurements were carried out in MeCN at -30°C . Luminescence spectra were recorded in distilled (but not degassed) MeCN solution using a Perkin-Elmer LS-50B luminescence spectrometer; the quantum yield of $[Ru(bipy)_2L][PF_6]_2$ was calculated by the method of Demas and Crosby,²¹ using $[Ru(bipy)_3]Cl_2$ in aerated water as a reference ($\phi = 0.028$).²²

The compounds $[Ru(bipy)_2Cl_2] \cdot 2H_2O$,²³ phenanthroline-5,6-dioxime⁸ and 5,6-diaminophenanthroline⁸ were prepared according to the published methods.

Syntheses

Dinuclear complex $[Ru(bipy)_2]_2(\mu\text{-pdi})[PF_6]_4$. A mixture of $[Ru(bipy)_2Cl_2] \cdot 2H_2O$ (0.30 g, 0.58 mmol) and dap (0.060 g, 0.20 mmol) in ethylene glycol (15 cm³) was heated to reflux for 12 h. The mixture was then allowed to cool, the solvent removed *in vacuo*, and water (100 cm³) added. The resulting solution was added to a column containing Sephadex SP-25 cation exchange resin in water, and eluted with aqueous NaCl solution. Initial elution with 0.3 M NaCl solution resulted in traces of the orange mononuclear complex $[Ru(bipy)_2(dap)]Cl_2$; then elution with 0.6 M NaCl solution gave the dinuclear complex $[Ru(bipy)_2]_2(\mu\text{-pdi})[PF_6]_4$. Addition of NH_4PF_6 to the aqueous solutions of the chloride salts of the complexes afforded precipitates of the hexafluorophosphate salts which were filtered off, washed with water, and dried. The yields were 15% of $[Ru(bipy)_2(dap)][PF_6]_2$ (identity confirmed by its ES mass spectrum: *m/z* 796, $\{Ru(bipy)_2(dap)(PF_6)\}^+$; 623, $\{Ru(bipy)_2(dap - H)\}^+$) and 40% of $[Ru(bipy)_2]_2(\mu\text{-pdi})[PF_6]_4$. Samples for analysis were recrystallised from aqueous acetone.

Characterisation data for $[Ru(bipy)_2]_2(\mu\text{-pdi})[PF_6]_4$: ES-MS *m/z* 1470, $\{M - PF_6\}^+$; 1325, $\{M - 2PF_6\}^+$ (Found: C, 40.7; H, 3.0; N, 9.3. $[Ru(bipy)_2]_2(\mu\text{-pdi})[PF_6]_4 \cdot 2Me_2CO$ requires C, 40.2; H, 3.0; N, 9.7%).

A sample of 100 mg of the dinuclear complex was separated into its diastereoisomers by chromatography on a 2 m long column of Sephadex SP-25, using 0.25 M aqueous sodium toluene-*p*-sulfonate as eluent. The slower-moving band was subsequently identified crystallographically as the homochiral ($\Delta\Delta/\Delta\Delta$) diastereoisomer; the faster-moving fraction is accordingly the heterochiral ($\Delta\Lambda/\Lambda\Delta$) diastereoisomer. After collecting the aqueous fractions, the complexes were precipitated by addition of NH_4PF_6 before being filtered off, washed with water, dried, and recrystallised from aqueous acetone. The two components were present in approximately equal amounts.

The isoimidazole ligand L. A solution of dap (0.10 g, 0.48 mmol) in ethanol (50 cm³) was added slowly *via* a dropping funnel to a mixture of acetone (2 cm³) and ethanol (50 cm³). The resulting solution was stirred in air at room temperature for 24 h and then evaporated to dryness. The brown residue was purified by chromatography on silica, using CH_2Cl_2 -MeOH- Et_3N (90:9:1) as eluent; the desired product is the fastest-moving component of the mixture. Evaporation to dryness afforded pure L as a pale brown solid (57% yield). ¹H NMR (300 MHz, CD_3OD): δ 9.00 (2 H, dd, *J* 1.7, 4.7; H^a), 8.71 (2 H, dd, *J* 1.8, 7.9; H^c), 7.70 (1 H, dd, *J* 4.7, 7.9 Hz; H^b) and 1.66 (6 H, s; Me). Found: C, 67.5; H, 5.0; N, 20.6. $C_{15}H_{12}N_4 \cdot H_2O$ requires C, 67.7; H, 5.3; N, 21.1%. EI-MS: *m/z* 248 [100%, M⁺].

Mononuclear complex $[Ru(bipy)_2L][PF_6]_2$. A mixture of the ligand L (20.1 mg, 81 μmol) and $[Ru(bpy)_2Cl_2] \cdot 2H_2O$ (100 mg, 1.92 mmol) in ethanol (20 cm³) was heated to reflux for 3 h in air. The solvent was removed *in vacuo*, the residue dissolved in water and introduced onto a Sephadex SP-25 column. The

Table 4 Crystallographic data for the two complexes

	[{Ru(bipy) ₂ } ₂ (μ-pdi)][ClO ₄] ₄ ·2.5H ₂ O	[Ru(bipy) ₂ L][PF ₆] ₂ ·2MeCN
Formula	C ₅₂ H ₄₅ Cl ₄ N ₁₂ O _{18.5} Ru ₂	C ₃₉ H ₃₄ F ₁₂ N ₁₀ P ₂ Ru
<i>M</i>	1477.94	1033.77
System, space group	Monoclinic, <i>C2/c</i>	Orthorhombic, <i>Aba2</i>
<i>a</i> /Å	29.300(8)	13.862(2)
<i>b</i> /Å	17.762(8)	15.622(2)
<i>c</i> /Å	22.139(8)	19.794(3)
β/°	97.19(2)	
<i>U</i> /Å ³	11431(7)	4287(1)
<i>Z</i>	8	4
μ/mm ⁻¹	0.802	0.536
Reflections collected:	29255, 10041, 0.0791	13053, 4809, 0.0184
total, independent, <i>R</i> _{int}		
Final <i>R</i> 1, <i>wR</i> 2 ^a	0.0712, 0.2130	0.0295, 0.0802

^a The value of *R*1 is based on selected data with a threshold of $F \geq 4\sigma(F)$; the value of *wR*2 is based on all data.

major red band was eluted using 0.3 M aqueous NaCl solution, and isolated as the hexafluorophosphate salt by precipitation with NH₄PF₆ to give clean [Ru(bipy)₂L][PF₆]₂. Yield: 60.1 mg, 78%. ¹H NMR (300 MHz, CD₃CN): δ 8.70 (2 H, dd, *J* 1.3, 7.9; H^a), 8.52 (4 H, d, *J* 8.3; bipy H³/H³), 8.09 (4 H, m, bipy H⁴/H⁴), 7.94 (2 H, dd, *J* 1.5, 5.5; H^a), 7.81 (2 H, d, *J* 5.7; bipy H⁶), 7.78 (2 H, d, *J* 5.7; bipy H⁶), 7.59 (2 H, dd, *J* 5.7, 8.1; H^b), 7.43 (2 H, ddd, *J* 1.5, 5.7, 7.7; bipy H⁵), 7.38 (1 H, ddd, *J* 1.4, 5.7, 7.6; bipy H⁵) and 1.64 (6 H, s). Found: C, 45.1; H, 3.1; N, 10.9. C₃₅H₂₈F₁₂N₈P₂Ru·acetone requires C, 45.2; H, 3.4; N, 11.1%. ES-MS: *m/z* 806, {*M* - PF₆}⁺; 663, {*M* - 2PF₆}⁺ and 331, {*M* - 2PF₆}²⁺.

X-Ray crystallography

Suitable crystals were quickly transferred from the mother-liquor to a stream of cold N₂ on a Siemens SMART diffractometer fitted with a CCD-type area detector. In both cases a full sphere of data was collected at -100 °C using graphite-monochromatised Mo-Kα radiation (λ 0.71073 Å). A detailed experimental description of the methods used for data collection and integration using the SMART system has been published.²⁴ Table 4 contains a summary of the crystal parameters, data collection and refinement. The absorption correction was applied using SADABS.²⁵ In both cases the structures were solved by conventional direct methods and refined by the full-matrix least-squares method on all *F*² data using the SHELXTL 5.03 package on a Silicon Graphics Indy computer.²⁶ Non-hydrogen atoms were refined with anisotropic thermal parameters; hydrogen atoms were included in calculated positions and refined with isotropic thermal parameters riding on those of the parent atom. Crystals of [Ru(bipy)₂L]-[PF₆]₂·2MeCN were grown by diffusion of ether vapour into a concentrated MeCN solution of the complex, and the structural determination presented no problems. The complex cation lies on a C₂ axis which passes through the Ru atom and also through C(43).

Crystals of [{Ru(bipy)₂}₂(μ-pdi)][ClO₄]₄·2.5H₂O were grown by slow evaporation of an aqueous acetonitrile solution. The crystal structure is complicated by substantial disorder of the bridging ligand, the perchlorate anions and the water molecules in the lattice. The bridging ligand is disordered over two orientations which involve interchanging the two binding sites, as described earlier (see Fig. 2). The atoms involved in the disorder are C(102), C(103), C(112) and C(113) (major component, 61% site occupancy) and C(202), C(203), C(212) and C(213) (minor component, 39% site occupancy); all other atoms of the bridging ligand and common to both components and were refined with 100% site occupancy. This disorder of the bridging ligand implies that there should be associated disorder of the terminal {Ru(bipy)₂}²⁺ fragments. This could not be resolved, no doubt because their geometries are almost identical, but it does

account for the slightly high thermal parameters (*ca.* 0.1 Å²) for a few of the bipyridyl carbon atoms.

Three of the perchlorate anions, which are close to the bridging ligand, are likewise disordered and were refined with fractional site occupancies as follows; for convenience these ions will be referred to by the number of the central Cl atom. Perchlorate ion 1 is well behaved with no disorder. The oxygen atoms of perchlorate ions 2 and 3 are each disordered over two closely-spaced positions with fractional site occupancies of 61 and 39% (matching the disorder of the bridging ligand). Perchlorate ion 4 is disordered over two closely spaced sites with 25% site occupancy in each, giving 50% occupancy in total, and perchlorate ion 5 has only 50% site occupancy for all atoms. Restraints were applied to both the geometric and thermal parameters of the disordered perchlorate anions. There are four additional oxygen atoms of water molecules [O(1) to O(4)], of which one has 100% site occupancy and the other three were assigned 50% site occupancy; hydrogen atoms were not included in the refinement for these. Overall, therefore, there are four perchlorate ions and 2.5 water molecules per dinuclear complex. The largest residual electron-density peaks, of intensity <1 e Å⁻³, are close to one of the disordered anions.

CCDC reference number 186/1556.

See <http://www.rsc.org/suppdata/dt/1999/2999/> for crystallographic files in .cif format.

Acknowledgements

We thank the EPSRC for financial support.

References

- J.-P. Sauvage, J.-P. Collin, J.-C. Chambron, S. Guillerez, C. Coudret, V. Balzani, F. Barigelli, L. De Cola and L. Flamigni, *Chem. Rev.*, 1994, **94**, 993; A. Harriman and R. Ziessel, *Chem. Commun.*, 1996, 1707; V. Balzani, A. Juris, M. Venturi, S. Campagna and S. Serroni, *Chem. Rev.*, 1996, **96**, 759; V. Balzani and F. Scandola, *Supramolecular Photochemistry*, Ellis Horwood, Chichester, 1991.
- M. D. Ward, *Chem. Soc. Rev.*, 1995, **24**, 121.
- F. M. MacDonnell and S. Bodige, *Inorg. Chem.*, 1996, **35**, 5758; S. Bodige, A. S. Torres, D. J. Maloney, D. Tate, G. R. Kinsel, A. K. Walker and F. M. MacDonnell, *J. Am. Chem. Soc.*, 1997, **119**, 10364; S. Campagna, S. Serroni, S. Bodige and F. M. MacDonnell, *Inorg. Chem.*, 1999, **38**, 692.
- N. C. Fletcher and F. R. Keene, *J. Chem. Soc., Dalton Trans.*, 1999, 683; N. C. Fletcher, P. C. Junk, D. A. Reitsma and F. R. Keene, *J. Chem. Soc., Dalton Trans.*, 1998, 133; T. J. Rutherford, O. van Gijte, A. Kirsch-De Mesmaeker and F. R. Keene, *Inorg. Chem.*, 1997, **36**, 4465; B. T. Patterson and F. R. Keene, *Inorg. Chem.*, 1998, **37**, 645.
- L. S. Kelso, D. A. Reitsma and F. R. Keene, *Inorg. Chem.*, 1996, **35**, 5144.
- P. Hayoz, A. von Zelewsky and H. Stoeckli-Evans, *J. Am. Chem. Soc.*, 1993, **115**, 5111; H. Muerner, P. Belser and A. von Zelewsky, *J. Am. Chem. Soc.*, 1996, **118**, 7989; H. Muerner, A. von Zelewsky

- and H. Stoeckli-Evans, *Inorg. Chem.*, 1996, **35**, 3931; N. C. Fletcher, F. R. Keene, H. Viebrock and A. von Zelewsky, *Inorg. Chem.*, 1997, **36**, 1113.
- 7 D. Tzalis and Y. Tor, *J. Am. Chem. Soc.*, 1997, **119**, 852; K. Wärnmark, P. N. W. Baxter and J.-M. Lehn, *Chem. Commun.*, 1998, 993.
 - 8 S. Bodige and F. M. MacDonnell, *Tetrahedron Lett.*, 1997, **38**, 8159.
 - 9 E. Ishow, A. Gourdon and J.-P. Launay, *Chem. Commun.*, 1998, 1909; E. Ishow, A. Gourdon, J.-P. Launay, P. Lecante, M. Verelst, C. Chiorboli, F. Scandola and C. A. Bignozzi, *Inorg. Chem.*, 1998, **37**, 3603; P. T. Gulyas, T. A. Smith and M. N. Paddon-Row, *J. Chem. Soc., Dalton Trans.*, 1999, 1325.
 - 10 W. Paw and R. Eisenberg, *Inorg. Chem.*, 1997, **36**, 2287; P. L. Hill, L. Y. Lee, T. R. Younkin, S. D. Orth and L. McElwee-White, *Inorg. Chem.*, 1997, **36**, 5655; G. Hilt, T. Jarbawi, W. R. Heineman and E. Steckhan, *Chem. Eur. J.*, 1997, **3**, 79.
 - 11 H. Masui, A. B. P. Lever and P. R. Auburn, *Inorg. Chem.*, 1991, **30**, 2404; H. Masui, A. B. P. Lever and E. S. Dodsworth, *Inorg. Chem.*, 1993, **32**, 258.
 - 12 D. A. Bardwell, J. C. Jeffery, E. Schatz, E. E. M. Tilley and M. D. Ward, *J. Chem. Soc., Dalton Trans.*, 1995, 825.
 - 13 K. E. Davies, G. E. Domany, M. Farhat, J. A. L. Herbert, A. M. Jefferson, M. de los A. Gutierrez Martin and H. Suschitzky, *J. Chem. Soc., Perkin Trans. 1*, 1984, 2465.
 - 14 Y. Xiong, X.-F. He, X.-H. Zou, J.-Z. Wu, X.-M. Chen, L.-N. Ji, R.-H. Li, J.-Y. Zhou and K.-B. Yu, *J. Chem. Soc., Dalton Trans.*, 1999, 19.
 - 15 A. Juris, V. Balzani, F. Barigletti, S. Campagna, P. Belser and A. von Zelewsky, *Coord. Chem. Rev.*, 1988, **84**, 85.
 - 16 J. Bolger, A. Gourdon, E. Ishow and J.-P. Launay, *Inorg. Chem.*, 1996, **35**, 2937.
 - 17 P. R. Auburn and A. B. P. Lever, *Inorg. Chem.*, 1990, **29**, 2551.
 - 18 K. H. Puthraya and T. S. Srivastava, *Polyhedron*, 1985, **4**, 1579; S. S. Kamath, V. Uma and T. Srivastava, *Inorg. Chim. Acta*, 1989, **166**, 91.
 - 19 G. A. Heath, L. J. Yellowlees and P. S. Braterman, *J. Chem. Soc., Chem. Commun.*, 1981, 287.
 - 20 S.-M. Lee, R. Kowallick, M. Marcaccio, J. A. McCleverty and M. D. Ward, *J. Chem. Soc., Dalton Trans.*, 1998, 3443.
 - 21 J. N. Demas and G. A. Crosby, *J. Phys. Chem.*, 1971, **75**, 991.
 - 22 K. Nakamura, *Bull. Chem. Soc. Jpn.*, 1982, **55**, 2697.
 - 23 B. P. Sullivan, D. J. Salmon and T. J. Meyer, *Inorg. Chem.*, 1978, **17**, 3334.
 - 24 P. L. Jones, A. J. Amoroso, J. C. Jeffery, J. A. McCleverty, E. Psillakis, L. H. Rees and M. D. Ward, *Inorg. Chem.*, 1997, **36**, 10.
 - 25 SADABS, A program for absorption correction with the Siemens SMART area-detector system, G. M. Sheldrick, University of Göttingen, 1996.
 - 26 SHELXTL 5.03 program system, Siemens Analytical X-Ray Instruments, Madison, WI, 1995.

Paper 9/03556G